J Mater Sci (2011) 46:5546–5552
DOI 10.1007/s10853-011-5501-0

Effects of heat treatments on the serrated flow in a Ni–Co–Cr-base superalloy

C. Y. Cui · T. Jin · X. F. Sun

Received: 10 February 2011 / Accepted: 22 March 2011 / Published online: 5 April 2011

Abstract Serrated flow in a Ni–Co–Cr-base superalloy was studied in three microstructural conditions (SUB, SUBA, and SUPER) from 25 to 750 °C by tensile test at initial strain rates ranging from 8×10^{-5} to 3×10^{-3} s^{-1}. The results showed that the SUB and SUBA samples had fine grain size of about 9 μm, whereas the SUPER samples had coarse grain size of about 600 μm. The tertiary γ' fraction was about 0 in the SUB, 5% in the SUBA, and 15% in the SUPER samples, respectively. The types and temperature ranges of serration were different in the alloy with SUB, SUBA, and SUPER microstructures. It is proposed that the tertiary γ' fraction and size had great effects on the serrated flow of the alloy with different microstructures.

Introduction

Serrated flow during plastic deformation is commonly observed in many alloys within a certain regime of temperature and strain rate. This serration in alloys, generally referred to as the Portevin–Le Chatelier (PLC) effect, is considered to be an instability associated with dynamic strain aging (DSA). The dynamic interaction between diffusing solute atoms and mobile dislocation during plastic flow is generally accepted to explain the observed phenomena [1].

DSA has also been observed in many nickel-base superalloys with different microstructures over a range of temperatures and strain rates [2–7]. For example, negative values of strain rate sensitivity and a PLC effect have been observed in aged Waspalloy [2, 3], Udimet720Li [4], and Inconel 718 [5–7]. Normal behavior, i.e., critical strain for serration (ε_c) increases with decreasing test temperature and increasing the strain rate, is often observed in these Ni-base superalloys. However, in peak aged Waspalloy [2], Udimet720Li [4], and Inconel718 [7], the inverse behavior, i.e., ε_c increases with increasing temperature and decreasing strain rate, is also found. Hayes et al. [2, 3] attributes the diffusion of interstitial C atoms forming an atmosphere around mobile dislocations to be responsible for serrated yielding in Waspalloy. They further suggest that the change from normal to inverse behavior should be a result of interactions between carbon atmospheres and the γ' strengthening precipitates. Gopinath et al. [4] suggest that the locking mobile dislocations by substitutional alloy elements (Cr, Co, Ti, Al, Mo, and W) would be responsible for the DSA in Udimet720Li. Hale et al. [7] have identified that the lattice diffusion of interstitial C atoms at lower temperatures (127–427 °C) and of substitutional Cr atoms at higher temperatures (477–627 °C) is responsible for serrated yielding in Inconel 718.

From the brief literature reviews, the following points appear: (i) most of the studies explains the mechanisms for DSA on the basis of the activation energy for diffusion of different solutes in the serrated regime and (ii) at low temperature, the diffusion of C atom is responsible for the DSA, while at high temperature, there is different opinion as to which element is responsible for DSA.

Recently, Cui et al. [8], from TEM observations on the tensile-deformed samples, suggest that the normal behavior should be associated with conventional DSA mechanism due to dynamic dislocation–solute interaction, while the inverse behavior would be related to the occurrence of

C. Y. Cui (✉) · T. Jin · X. F. Sun
Superalloys Division, Institute of Metal Research (IMR), Chinese Academy of Sciences, 72 Wenhua Road, Shenyang 110016, China
e-mail: chycui@imr.ac.cn

stacking faults (SF) in a Ni–Co-base superalloy. The microstructures of the Ni–Co-base superalloy [9–12] are complex: it mainly consists of γ grain, primary γ', secondary γ', tertiary γ', and carbide/boride on grain boundary. These microstructural parameters can be generally controlled by heat treatment, cooling rate, and aging [10, 12]. Mukherji et al. [13] and Viswanathan et al. [14] have reported that applied stress and precipitate size can significantly affect the creep rates and the deformation modes in the superalloys IN738LC and Rene88DT. However, a systematic study on the effect of the size and fraction of γ' precipitate on DSA has not been addressed fully in the literature. In this work, we focus on the effect of microstructural scale, particularly the size and fraction of tertiary γ' precipitate, on the DSA of the Ni–Co–Cr-base superalloy with high-Co content. We identify the serrated flow in three microstructural conditions and propose an explanation for the effect of microstructural variation on the DSA.

Experimental procedure

The chemical composition (in wt%) of the alloy was 0.01Ce, 0.02C, 13.6Cr, 23Co, 2.8Mo, 1.2W, 5.6Ti, 2.3Al, 0.02B, 0.03Zr, and Ni balance. The alloy was homogenized at 1,200 °C for 10 h and subsequently hot extruded to 30 mm in diameter. Here, we define the primary γ' as the undissolved γ' particle during the solution stage, secondary γ' as the intragranular γ' with particle diameter between 50 and 100 nm, and tertiary γ' as intragranular γ' with particle diameter below 50 nm. As shown in Fig. 1a, the as-extruded alloy mainly consisted of equiaxed γ grain and high density of primary γ'. The inset in Fig. 1a showed intragranular secondary γ' precipitate and tertiary γ' precipitate. The variation of grain size and fraction of primary γ' with the solution temperature is plotted in Fig. 1b. The solvus temperature of γ' was determined to be about 1,150 °C. The increase of solution temperature resulted in the decrease of primary γ' fraction, which indicated the increase of secondary and tertiary γ' fraction [10]. Thus, the tertiary γ' fraction could be controlled by suitable heat treatment and cooling rate. The samples were then heat treated to produce three different microstructures: (i) subsolvus solution treated at 1,110 °C for 4 h and water cooling (WC), designated as SUB; (ii) SUB alloy aged at 650 °C for 24 h and 760 °C for 16 h to precipitate secondary and tertiary γ', designated as SUBA; (iii) supersolvus solution treated at 1,200 °C for 4 h and then aged at 650 °C for 24 h and 760 °C for 16 h to dissolve all the γ' and re-precipitate the γ', designated as SUPER.

Tensile tests were performed on the samples with a gage section of 3 mm in diameter and 20 mm in length. Tensile tests were performed on a Shimadz AG-25KNE machine at temperatures ranging from 25 to 750 °C and initial strain rates ranging from 3×10^{-3} to 8×10^{-5} s^{-1}, respectively. All the tests were started after holding the specimens for 20 min at the temperature tested. Fracture surfaces were observed by scanning electron microscopy (SEM) in a JSM-6301F microscope. The transmission electron microscopy (TEM) disks with thickness of about 0.3 mm were cut from the samples perpendicular to the tensile axis. Thin foils for TEM observations were prepared by means of a standard twin jet polishing technique in a solution of 23% perchloric acid and 77% acetic acid at about −30 °C. TEM observations were carried out on a Philips CM200 operated at 200 kV.

Results

Microstructures

The γ' solvus temperature of the alloy was determined to be about 1,150 °C (Fig. 1b). Thus, the SUB and SUBA samples were the subsolvus heat treatment, while the SUPER samples belonged to the supersolvus heat treatment. Figure 2 shows the microstructures of the alloys after heat treatments. The SUB and SUBA samples consisted of

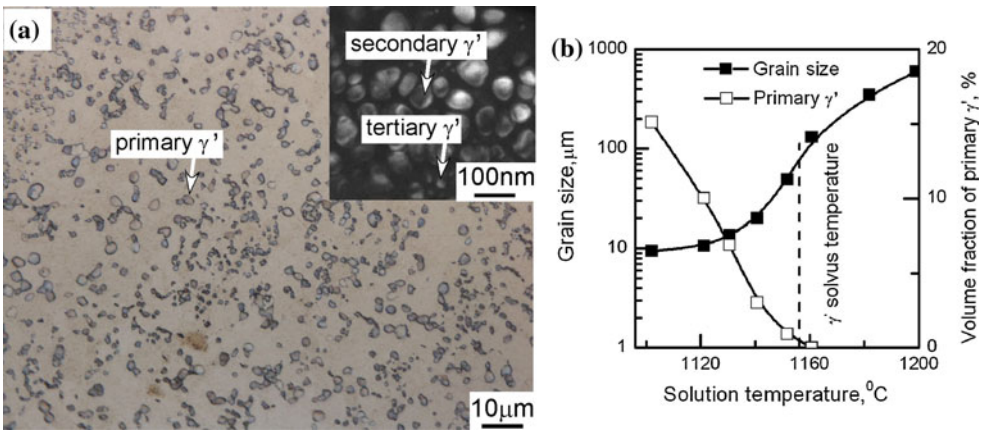

Fig. 1 **a** The microstructures of the as-extruded alloy and **b** the variation of grain size and primary γ' fraction with solution temperature

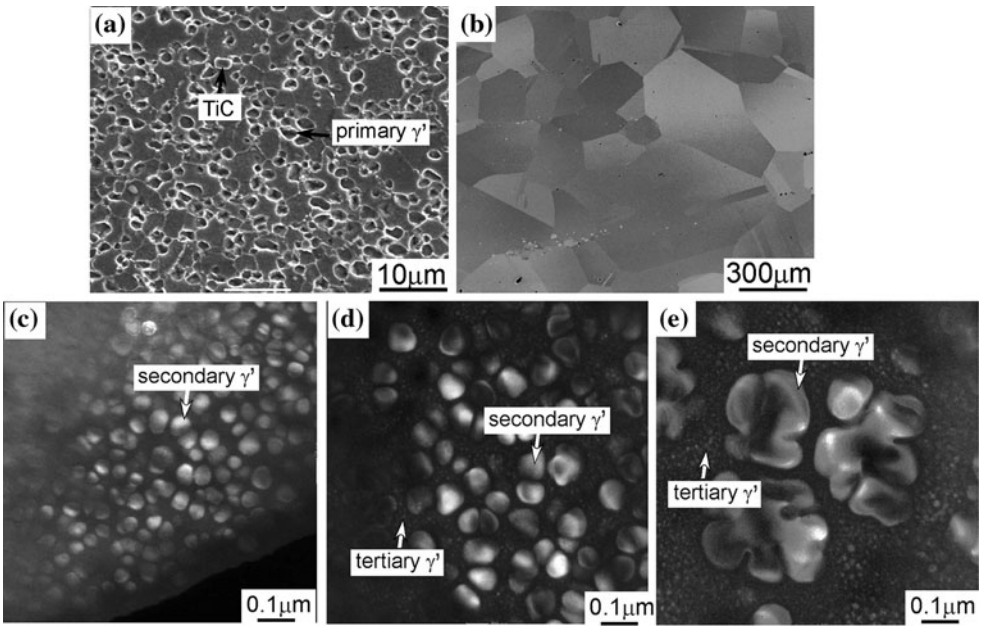

Fig. 2 Representative microstructures of the Ni–Co–Cr-base superalloy: **a**, **c** SUB; **a**, **b** SUBA; and **b**, **e** SUPER. (**a**) and (**b**) are scanning electron microscope, while (**c**–**e**) are transmission electron microscopes

Table 1 Effects of heat treatment conditions on the microstructural parameters (grain size, primary, secondary, and tertiary γ')

Phase	Grain size (μm)	Primary γ' fraction	Secondary γ'		Tertiary γ'	
			Fraction	Size (nm)	Fraction	Size (nm)
SUB	9.0	0.15	~0.30	~70	–	–
SUBA	9.0	0.15	~0.25	~80	~0.05	~15
SUPER	600	0	~0.30	~300	~0.15	~20

equiaxed γ grain (about 9 μm), high fraction of primary γ' precipitate (15%) at the grain boundary of the γ grain and small amounts of TiC (Fig. 2a), whereas the SUPER sample had coarse grain size of about 600 μm and no primary γ' precipitate, due to the supersolvus heat treatment (Fig. 2b). At higher magnification, typical microstructures in three microstructural conditions are shown in Fig. 2c–e. The SUB microstructure (Fig. 2c) revealed a sparse distribution of secondary γ' precipitate [8]. The average size of secondary γ' was measured to about 70 nm. No tertiary γ' precipitates were detected by dark field (DF) TEM observations, thus the tertiary γ' fraction was considered to be zero. In addition to the secondary γ', some fine tertiary γ' precipitate, which formed by aging at 650 and 760 °C [15], were clearly observed in the SUBA sample (Fig. 2d). Large secondary γ' precipitate and uniformly distributed tertiary γ' precipitate were observed in the SUPER microstructure (Fig. 2e).

As the size of tertiary γ' was very fine, the tertiary γ' fraction was approximately estimated by using the following equation:

$$V_{\text{tertiary }\gamma'} = V_{\text{total }\gamma'} - V_{\text{primary }\gamma'} - V_{\text{secondary }\gamma'} \quad (1)$$

The $V_{\text{total }\gamma'}$ was calculated to be about 45% at 700 °C by using Thermo-Calc software with a commercial database (Ni-data7). The primary and secondary γ' fractions were measured by using a point counting method [10]. The tertiary γ' fraction was estimated to be about 5% in the SUBA sample and 15% in the SUPER sample, respectively. All the obtained results are summarized in Table 1.

Mechanical properties

Figure 3a–d shows the true stress–strain curves of the SUB, SUBA, and SUPER samples tested at temperatures ranging from 25 to 750 °C and an initial strain rate of 3×10^{-4} s^{-1}. As shown in Fig. 3a, in the SUB sample, serrated stress–strain curves resulting from periodic stress jumps in the plastic regime were observed at test temperatures ranging from 300 to 550 °C, typically at 400 °C. The stress–strain curves at temperatures out of this range

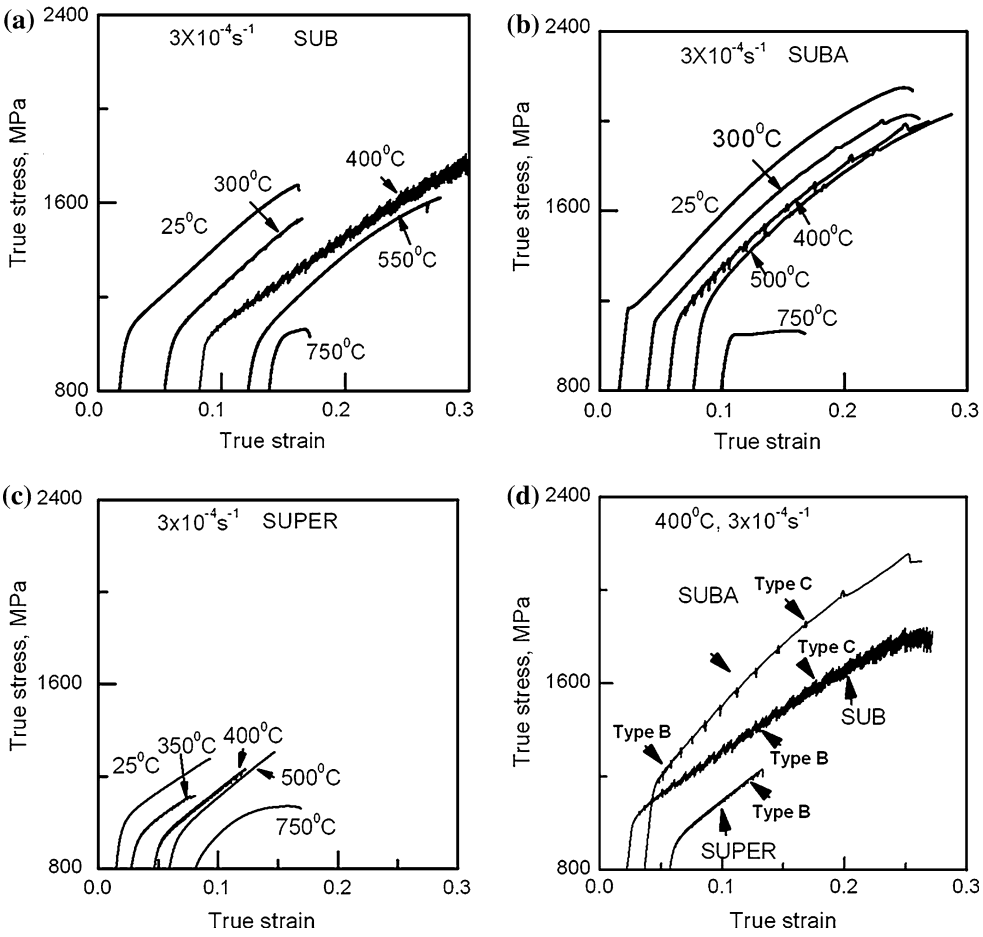

Fig. 3 Typical true stress–strain curves for different microstructures at 3×10^{-4} s^{-1} **a** SUB, **b** SUBA, and **c** SUPER. (**d**) Comparison of the true stress–strain curves of the alloy with SUB, SUBA, and SUPER microstructures at 400 °C

were smooth. In the SUBA sample, the serrated stress–strain curves were found in the temperatures ranging from 300 to 500 °C (Fig. 3b). In the case of SUPER sample (Fig. 3c), the serrated stress–strain curves were found in the temperature range of 300–450 °C. In addition to the temperature range difference of serrated flow, some differences in serration type could also be noticed for the SUB, SUBA, and SUPER microstructures, as shown in Fig. 3d. Type A, B, and C serrations were observed in the SUB and SUBA samples within most of the temperatures and strain rates studied, while the magnitude of Type B serrations was smaller in the SUBA sample than that in the SUB sample. However, only Type B serration was observed in the SUPER sample. The occurrences of serration and their type were closely related to the microstructures, which will be discussed later.

Figure 4a shows the variation of yield stress of the SUBA and SUPER samples with the test temperatures ranging from 25 to 750 °C at a strain rate of 3×10^{-4} s^{-1}. In general, the SUBA samples had higher yield stress than the SUPER samples, due to its fine grain size, as listed in Table 1. On the other hand, in the SUBA and SUPER samples, the yield stress was slightly affected by temperatures ranging from 25 to 600 °C, and decreased gradually at temperature above 600 °C. As shown in Fig. 4b, the SUBA sample possessed the large elongation than the SUPER sample at temperatures below 600 °C. Specifically, the total elongations of the SUBA samples were slightly affected by temperatures below 600 °C and decreased markedly at temperatures above 600 °C. This tendency was different from that in Udimet720Li alloy [4]. In contrast, the elongation of the SUPER samples was slightly affected by temperatures from 25 and 750 °C.

Microstructures associated with serrated flow

Fractographic observations and stress–strain curves (Fig. 3) showed that no necking happened before fracture in the DSA regime. Fracture surfaces of the SUB, SUBA, and SUPER samples are shown in Fig. 5. The SUB and SUBA samples (Fig. 5a, b) showed the presence of equiaxed dimples, indicating the ductile mode of fracture in both the cases. In the SUPER samples (Fig. 5c), the fracture mode was a mixture of intergranular and transgranular fracture. These observations showed that characteristics of fracture in the SUB and SUBA microstructure were

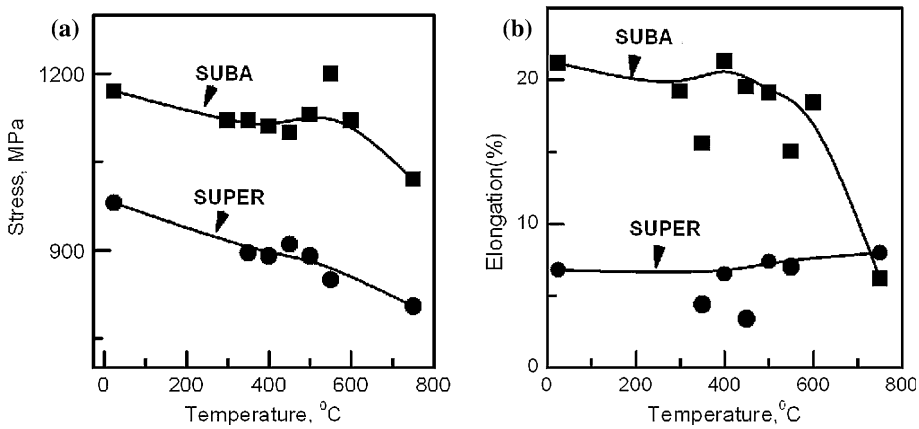

Fig. 4 The variation of **a** yield stress and **b** elongation in the SUBA and SUPER samples with the test temperatures ranging from 25 to 750 °C

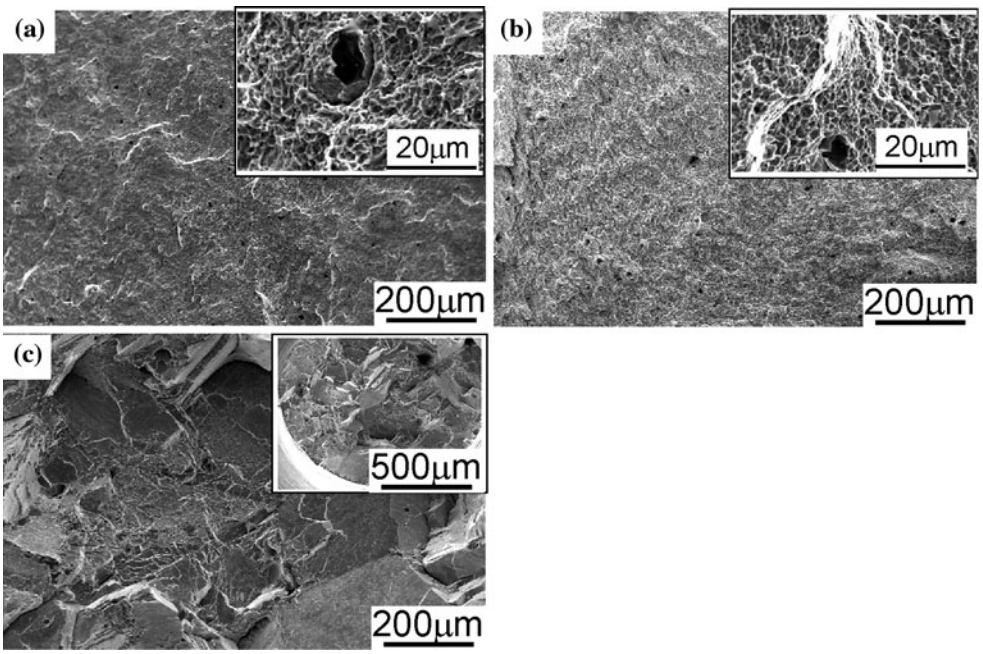

Fig. 5 Fractographs of the Ni–Co–Cr-base superalloy with **a** SUB, **b** SUBA, and **c** SUPER microstructures tested at 400 °C, 3×10^{-4} s^{-1}

different from those in the SUPER microstructure, mainly due to the grain size effect on ductility (9 μm in the SUBA sample vs. 600 μm in the SUPER sample).

TEM observations were also carried out to understand the different deformation mechanism in the SUB and SUBA samples. In the SUB sample, as shown in Fig. 6a, the dislocations were very long, implying that they were not pinned by fine γ' precipitate, thus they moved easily. In addition, short SF were present in the SUB samples, and were hindered by the secondary γ' precipitate. The characteristics of SF were different from those reported in Ref. [8]. In contract, in the SUBA sample, the dislocations cells formed in plastic deformation. The cell walls with a high density of dislocations were rather chaotic regions, while the cell interior had relatively fewer dislocations, as shown in Fig. 6b. This phenomenon indicated that the dissociation of the matrix perfect dislocation was difficult, so the cross-slip became relatively easier.

Discussion

It turned out that the size and fraction of γ' of the Ni–Co–Cr-base superalloy significantly changed during heat treatment with the evolution of grain growth, and that the serrated flow was affected by different microstructural conditions. That is, Type A, B, and C serrations were observed in the alloy with fine grain size (SUB and SUBA samples). In contrast, only Type B serration was observed in the alloy with coarse grain size (SUPER sample).

As shown in Fig. 2 and Table 1, grain size, fraction of primary γ', size and fraction of secondary and tertiary γ',

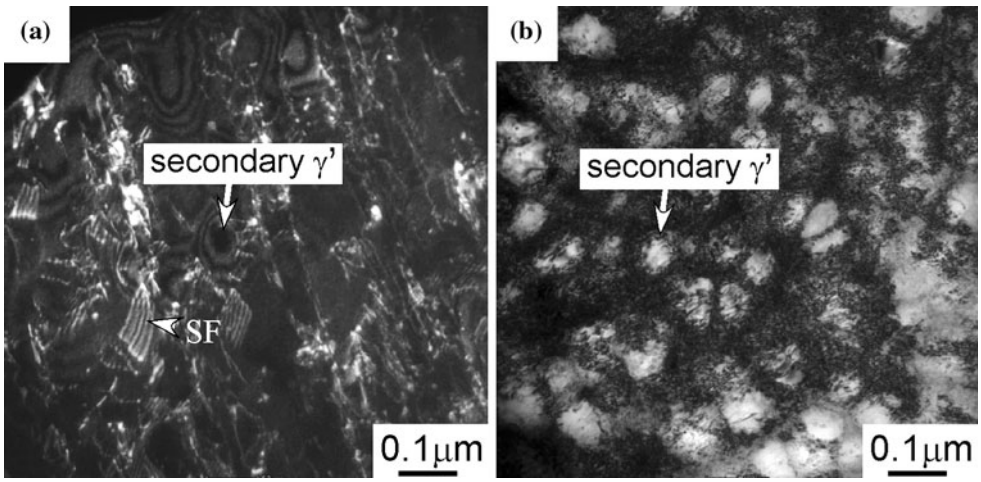

Fig. 6 TEM observations on the deformed Ni–Co–Cr-base superalloy with **a** SUB and **b** SUBA microstructures tested at 400 °C, 3×10^{-4} s^{-1}

and substitutional element content changed simultaneously during the heat treatment. Among these parameters, size and fraction of tertiary γ' was probably the main contributing factor to DSA of the alloy with different microstructures because of the following reasons. First, the main difference of the SUB and SUBA samples was the tertiary γ', i.e., tertiary γ' was observed not in the SUB sample, but in the SUBA samples; second, the dislocations moved easily in the SUB sample without tertiary γ', as shown in Fig. 6a. Type B was very small magnitude in the SUBA sample (Fig. 3c), which disappeared at higher strain because of the interaction of tertiary γ' with mobile dislocations; third, the fraction of tertiary γ' in the SUBA sample was greatly different from that in the SUPER samples, as listed in Table 1, thus the temperature range and serration type were different (Fig. 3). Regarding the tertiary γ' effect in superalloy, Viswanathan et al. [14] have experimentally confirmed by using conventional and high-resolution TEM that the tertiary γ' volume fraction is crucial in dictating the transition in creep mechanism.

We can also understand the tertiary γ' effect in DSA by using the critical strain to serration. It is known that in the precipitate strengthened materials, the critical strain to serration is often related to the average spacing between particle [16, 17] and can be described by:

$$\varepsilon_c^m = B L^{-1} \dot{\varepsilon}_c \exp(Q_m/kT) \quad (1)$$

Here, B is constant, $\dot{\varepsilon}_c$is the plastic strain rate, Q_m is the effective energy for the thermally activated process, k and T have their usual meanings and m is a constant equal to 0.5–1.0 for nickel-base alloys. The particle spacing, L, is related to the volume fraction of γ' and mean planar cross-section of a particle in the slip plane. The SUBA sample has smaller L than the SUB sample, due to the tertiary γ' precipitation during aging, as shown in Fig. 2. Thus, the critical strains to serration were measured to be 0% in the SUB sample and 0.2% in the SUBA sample (Fig. 3c), respectively. In this study, only Type B serration was observed in the alloy with coarse grain size. It is known that Type B serration corresponds to a hopping propagation of local band in the localized band in the axial direction of tensile specimen [18]. Type B serrations, which are also considered locking serrations, fluctuate about the mean flow curve in very quick succession. There were two possible reasons for the occurrence of Type B in the alloy with coarse grain size. One was related to the high content of tertiary γ' precipitates distributed uniformly in SUPER samples, the interaction of mobile dislocation with tertiary γ' became easier. Another was probably due to the coarse grain size. The effect of grain boundary on DSA was minimal in the SUPER samples with grain size of 600 μm.

The temperature ranges of serrations in the alloys with different microstructures were generally interpreted in the literature to be due to the formation of an atmosphere around dislocations and various elements [2–6]. At low temperature, the diffusion of interstitial C atom is generally believed to be responsible for the serrated phenomenon. Thus, the starting temperature of serrated flow was about 300 °C for the Ni–Co–Cr alloy with different microstructures. While at higher temperature, the interaction of substitutional elements with mobile dislocation is believed to be responsible for the DSA. During heat treatment, the content of substitutional solute atoms changes, due to these solutes becoming tied up as high fraction of tertiary γ' precipitate. Therefore, the disappearance temperature of serration was different in the alloy with different solute atom contents.

Next, we discussed the SFs observed in Fig. 6a. It is generally known that, in fcc metals, the stacking fault energy (SFE) is one of the important parameters determining which deformation and transformation mechanisms will occur during plastic deformation. Consequently, the SFE can affect strongly the mechanical properties of fcc metals. At low SFE metal, wide dissociation of dislocation

into Shockley partials can hinder dislocation glide and thus favors SFs or mechanical twinning [19]. The present alloy had a low SFE of about 25 mJ/m^2, mainly due to the high-Co content (23 wt%) [20]. Thus, the SFs could be observed in the present alloy with a low SFE.

Conclusions

The serrated flows were examined in the Ni-base superalloy from 25 to 750 °C by tensile test at initial strain rates ranging from 8×10^{-5} to 3×10^{-3} s^{-1} and the following results were obtained:

(1) The SUB and SUBA samples had fine grain size of 9 μm, whereas the SUPER samples had coarse grain size of about 600 μm. The tertiary γ' fraction was 0% in the SUB, 5% in the SUBA and 15% in the SUPER samples, respectively.

(2) The serrated flow was noticed at temperatures of 300–550 °C for the SUB sample, of 300–500 °C for the SUBA sample, and of 300–450 °C for the SUPER sample, respectively. Temperature did not influence tensile properties such as yield stress, elongation, and fracture features in the DSA regime.

(3) The results showed that the fraction and size of tertiary γ' probably had great influence on the serrated flow of the alloy, due to its interaction with the mobile dislocation.

Acknowledgements This work was financially supported by "Hundreds of Talents Project" and National Basic Research Program (973 Program) of China under grant No. 2010CB631200 (2010CB631206).

References

1. Rodriquez P (1984) Bull Mater Sci India 6:653
2. Hayes RW, Hayes WC (1982) Acta Metall 30:1295
3. Hayes RW (1983) Acta Metall 3(1):365
4. Gopinath K, Gogia AK, Kamat SV, Ramamurty U (2009) Acta Mater 57:1243
5. Chen W, Chaturvedi MC (1997) Mater Sci Eng A229:163
6. Nalawade SA, Sundararaman M, Kishore R, Shah JG (2008) Scr Mater 59:991
7. Hale CL, Rollings WS, Weaver ML (2001) Mater Sci Eng A 300:153
8. Cui CY, Gu YF, Yuan Y, Harada H (2011) Scr Mater 64:502
9. Cui CY, Gu YF, Harada H, Sato A (2005) Metall Mater Trans A 36:2921
10. Cui CY, Gu YF, Ping DH, Harada H (2009) Metall Mater Trans A 40:282
11. Gu YF, Cui C, Ping D, Harada H, Fukuda T, Fujioka J (2009) Mater Sci Eng A 510–511:250
12. Cui CY, Gu YF, Harada H, Ping DH, Sato A (2006) Metall Mater Trans A 37:3183
13. Mukherji D, Jiao F, Wahi RP (1991) Acta Metall Mater 39(7):1515
14. Viswanathan GB, Sarosi PM, Henry MF, Whitis DD, Milligan WW, Mills MJ (2005) Acta Mater 53:3041
15. Jackson MP, Reed RC (1999) Mater Sci Eng A 259:85
16. Sleeswyk AW (1958) Acta Metall 6:598
17. Lloyd DJ, Chung DW, Chaturvedi MC (1975) Acta Metall 23:93
18. Jiang H, Zhang Q, Chen X, Chen Z, Jiang Z, Wu X, Fan J (2007) Acta Mater 55:2219
19. Yuan Y, Gu YF, Cui CY, Osada T, Yokokawa T, Harada H (2011) Adv Eng Mater 13:296
20. Yuan Y, Gu YF, Cui CY, Osada T, Tetsui T, Yokokawa T, Harada H. J Mater Res (revised)